

See discussions, stats, and author profiles for this publication at: <https://www.researchgate.net/publication/228877726>

Folding of Intramolecular DNA Hairpin Loops: Enthalpy–Entropy Compensations and Hydration Contributions

ARTICLE *in* THE JOURNAL OF PHYSICAL CHEMISTRY B · SEPTEMBER 2002

Impact Factor: 3.3 · DOI: 10.1021/jp0260853

CITATIONS

14

READS

24

5 AUTHORS, INCLUDING:



Luis A Marky

University of Nebraska at Omaha

166 PUBLICATIONS 7,291 CITATIONS

SEE PROFILE

Folding of Intramolecular DNA Hairpin Loops: Enthalpy–Entropy Compensations and Hydration Contributions

Dionisios Rentzeperis,[†] Ronald Shikiya, Souvik Maiti, James Ho, and Luis A. Marky*

Departments of Pharmaceutical Sciences and Biochemistry and Molecular Biology and Eppley Institute for Cancer Research and Allied Diseases, University of Nebraska Medical Center, Omaha, Nebraska 68198-6025

Received: May 7, 2002

DNA intramolecular hairpins are appropriate models for the thermodynamic description of the pseudo-intramolecular melting behavior of native DNA. To improve our understanding of the stability and melting behavior of DNA secondary structures and of the physical properties of nucleic acids, we have carried out a thermodynamic investigation of all possible bulges and mismatches in the hairpin molecule: d(GCNGCT5GCGC) and d(GCNGCT5GCMGC), where *N* represents a bulged base and *N-M* represents a W-C or mismatched base pair. We used circular dichroism spectroscopy to determine the overall conformation of each hairpin and UV melting and differential scanning calorimetry techniques to characterize their unfolding thermodynamics. The majority of hairpins melted in two-state monophasic transitions with transition temperatures independent of strand concentration. Relative to the host hairpin with 4 dG-dC base pairs in the stem, all hairpins with a bulge or a mismatch are less stable, while the hairpins with an extra canonical base pair are more stable. In both cases, the effects are enthalpy driven, indicating a loss or gain in base-pair stacking interactions, respectively. We also obtained linear enthalpy–entropy compensations with slopes (or compensating temperatures) of 317 K (hairpins with lesions) and 395 K (hairpins with fully paired stems) which are indicative of processes that are driven by solute–solvent interactions. These compensating temperatures are in excellent agreement with the results of similar analysis of data sets of other laboratories. Therefore, the relative change in enthalpy contribution for a given hairpin is partially compensated by a change in their overall hydration. These results suggest that the inclusion of bulges and mismatches immobilizes additional structural water while the addition of a W-C base pair immobilizes electrostricted water.

Introduction

The presence of conserved palindromic sequences in non-coding regions of the genome indicates that hairpin structures are involved in gene regulation. For instance, plasmids under superhelical stress fold into cruciform structures,^{1–3} and in one of their folding pathways a hairpin intermediate is formed just before branch migration.⁴ However, there is still little evidence for their frequency of appearance, their stability *in vivo*, and their true biological significance. Several NMR and X-ray crystallographic investigations^{5–12} of synthetic DNA hairpins have shown that the 4–6 base-pairs stem adopts the “B” conformation while the loops of 4–5 nucleotides form constrained random coils that varies with the sequence.

Our understanding of the molecular forces that govern DNA and RNA secondary structures has increased considerably but a full thermodynamic description for the folding of hairpin loops is still needed.^{13–19} Short DNA hairpins are good thermodynamic models to mimic the pseudo-first-order unfolding transitions of natural DNA polymers because their intramolecular transitions take place in an all-or-none fashion at convenient experimental temperatures.¹⁷

The exposure of DNA to physical forces and mutagens or errors during replication results in DNA damage; examples include the incorporation of unpaired bases (bulges) and base-

pair mismatches.^{20,21} Bulges can promote frame shift mutations according to a mechanism proposed by Streisinger,²² while mismatches cause transitional and transversal mutations.²³ A complete understanding of the mechanisms of mutations not only includes the study of the structure of duplexes containing bulges and mismatches but also requires a detailed description of the energetic contributions.

The solvent accessible surface of DNA duplexes is primarily hydrophilic while nucleotide loops have a hydrophobic (aromatic bases) and a hydrophilic surface (sugar–phosphate backbone). This involves the immobilization of two types of hydrating water, electrostricted (around charged groups) and hydrophobic or structural (around polar and nonpolar groups).^{24–26} Therefore, the hydration properties of hairpin loops are expected to be between those of the standard B-DNA duplex and random coil conformations. In addition, the exposure of bases, and methyl groups of thymine loops, to the solvent could potentially immobilize additional structural water.

In this work, we report a thermodynamic investigation of two sets of single-stranded hairpins with sequences (i) d(GCNGCT5-GCGC), where *N* is a nonpaired base, and (ii) d(GCNGCT5-GCMGC), where *N-M* is a mismatch or a W-C base pair. We used melting protocols to characterize their helix-coil transitions. Relative to the host hairpin with 4 dG-dC base pairs, all hairpins with a bulge or a mismatch base pair are less stable while the hairpins with an extra canonical W-C base pair are more stable. The overall effect is enthalpy driven and indicates a loss or gain, respectively, in base-pair stacking interactions. We obtained

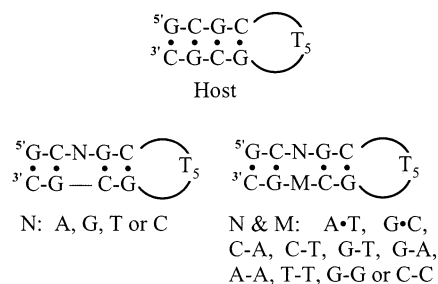
* To whom correspondence should be addressed. Tel: (402) 559-4628. Fax: (402) 559-9543. E-mail: lmarky@unmc.edu.

[†] Present address: 3-Dimensional Pharmaceuticals, Inc., Three Lower Makefield Corporate Center, 1020 Stony Hill Road, Yardley, PA 19067.

TABLE 1: Thermodynamic Parameters for the Helix-Coil Transition of Hairpins^a

| | UV spectroscopy | | | differential scanning calorimetry | | | | |
|-------------------------------------|-----------------|--------------------------------------|-------------|-----------------------------------|--------------------------------------|---------------------------------------|----------------------------------------|----------------------------------------|
| | T_M (°C) | ΔH_{vH} (kcal/mol) | Hyp. (%) | T_M (°C) | ΔH_{vH} (kcal/mol) | ΔH_{cal} (kcal/mol) | $T\Delta S_{\text{cal}}$ (kcal/mol) | ΔG°_{293} (kcal/mol) |
| hairpins with W-C base pairs | | | | | | | | |
| host | 76.4 | 35 | 19 | 75.3 | 34 | 34.9 | 29.4 | −5.5 |
| C•G | 81.6 | 45 | 21 | 83.2 | 43 | 43.2 | 35.5 | −7.7 |
| A•T | 74.9 | 39 | 18 | 74.6 | 39 | 39.3 | 33.1 | −6.2 |
| hairpins with bulges | | | | | | | | |
| A | 66.0 | 29 | 18 | 67.7 | 30 | 29.7 | 25.5 | −4.2 |
| C | 67.8 | 30 | 17 | 69.6 | 29 | 24.6 | 21.0 | −3.6 |
| G | 58.3 | 25 | 21 | 62.5 | 26 | 26.0 | 22.7 | −3.3 |
| T | 58.0 | 25 | 18 | 57.5 | 25 | 23.6 | 20.9 | −2.7 |
| hairpins with mismatched base pairs | | | | | | | | |
| A-G | 66.2 | 30 | 20 | 67.8 | 30 | 29.0 | 24.9 | −4.1 |
| T-G | 60.0 | 34 | 24 | 61.1 | 32 | 33.7 | 29.6 | −4.1 |
| T-T | 56.9 | 32 | 23 | 58.0 | 34 | 34.5 | 30.5 | −4.0 |
| C-C | 51.1 | 20 | 19 | 54.5 | 23 | 36.6 | 32.7 | −3.9 |
| C-A | 54.2 | 25 | 20 | 54.1 | 25 | 35.4 | 31.7 | −3.7 |
| G-G | 56.6 | 24 | 19 | 58.7 | 30 | 30.3 | 26.8 | −3.5 |
| A-A | 56.6 | 23 | 16 | 57.4 | 26 | 25.3 | 22.4 | −2.9 |
| C-T | 50.1 | 26 | 21 | 50.6 | 27 | 26.9 | 24.4 | −2.5 |

^a All values obtained in 10 mM phosphate, 0.1 mM Na₂EDTA, 1.0 M NaCl at pH 7.0. Experimental errors for each parameter, indicated in parentheses, as follows: T_M (± 0.5 °C), ΔH_{vH} ($\pm 15\%$), ΔH_{cal} ($\pm 3\%$), ΔS ($\pm 3\%$), and ΔG°_{293} ($\pm 5\%$).

**Figure 1.** Sequences of oligonucleotides and their designations.

enthalpy–entropy compensations with compensating temperatures that are characteristic of processes driven by solute–solvent interactions.

Experimental Section

Oligonucleotides were synthesized on an ABI 391-A automated DNA synthesizer or by the Synthetic Core facility at UNMC, using standard phosphoramidite chemistry as described previously.²⁷ All oligonucleotides were purified by HPLC using a salt gradient (0 to 1.0 M NaCl) on a C-18 column (Zorbax, Dupont), desalted on a G-10 Sephadex column, and lyophilized to dryness. The control hairpin, d(GCGCT₅GCGC), was designated as “host” and the hairpins with bulges or mismatches by the appropriate guest substitution, that is, “T” for d(GCTGCT₅GCGC) and “T-T” for d(GCTGCT₅GCTGC), see Figure 1. The molar extinction coefficient of each oligonucleotide was calculated in water at 260 nm using procedures reported previously.²⁸ The extinction coefficients at 95 °C, in mM^{−1} cm^{−1}, are as follows: host, 108; C, 115; A, 120; G, 118; T, 115; C•G, 125; A•T, 128; A-G, 131; T-G, 125; G-G, 128; T-T, 123; A-A, 133; C-C, 122; C-A, 128; and C-T, 122. All other chemicals were reagent grade. The buffer solutions consisted of 10 mM sodium phosphate 0.1 mM Na₂EDTA, adjusted to the desired ionic strength with NaCl.

The global conformation of each molecule was examined by circular dichroism spectroscopy. All CD spectra were collected on an AVIV 60DS spectrometer from 340 to 200 nm at 1-nm steps; the final spectrum corresponds to the average of at least three scans. Absorbance values of 0.7–0.8 were used with 1-cm

quartz cells. The temperature of the cell was kept constant at 20 °C with a Hewlett–Packard 891000-A temperature controller.

Absorption versus temperature profiles (melting curves) were obtained with a thermoelectrically controlled UV/Vis Perkin–Elmer 552 or Perkin–Elmer Lambda-10 spectrophotometers. The temperature was scanned at a heating rate of ~ 1.0 °C/min. Analysis of the equilibrium melting curves yielded the helix-coil transition temperature, T_M , and van’t Hoff enthalpy, ΔH_{vH} , as reported previously.²⁹

The unfolding heats of each hairpin were measured with the MC-2 differential scanning calorimeter from Microcal Inc. (Northampton, MA). Typically, a DNA solution was scanned against a buffer solution from 5 to 107 °C, normalized by the heating rate of 0.75 °C/min, and a buffer versus buffer scan subtracted and normalized by the effective number of moles used. Integration of the resulting curve, $\int \Delta C_p dT$, yields model-independent enthalpies, ΔH_{cal} . The ΔS_{cal} was obtained by a similar integration, $\int (\Delta C_p/T) dT$, and checked against a standard relationship for intramolecular transitions: $\Delta S_{\text{cal}} = \Delta H_{\text{cal}}/T_M$.²⁹ In the measurement of these terms, it is assumed that the duplex and random coil states have similar heat capacities. The free energy at any temperature T is obtained with the Gibbs relationship: $\Delta G^{\circ}_{\text{cal}}(T) = \Delta H_{\text{cal}} - T\Delta S_{\text{cal}} = \Delta H_{\text{cal}}(1 - T/T_M)$. Furthermore, the nature of the helix-coil transition is inspected by the $\Delta H_{\text{vH}}/\Delta H_{\text{cal}}$ ratio; a value of nearly one indicates a two-state transition.²⁹

Results and Discussion

In the unfolding of single-stranded hairpins, the T_M is expected to be independent of strand concentration; therefore, the unfolding of these molecules was studied as a function of strand concentration. UV melting curves at 275 nm were obtained over a twelvefold strand concentration range, 4–50 μM , and the calorimetric melting curves were performed at much higher strand concentrations (~ 300 μM). The UV melting (data not shown) of these molecules occurs in broad monophasic transitions with average hyperchromicities of 20%, see Table 1. Typical DSC scans are shown in Figure 2; these curves also show monophasic transitions with negligible changes in heat

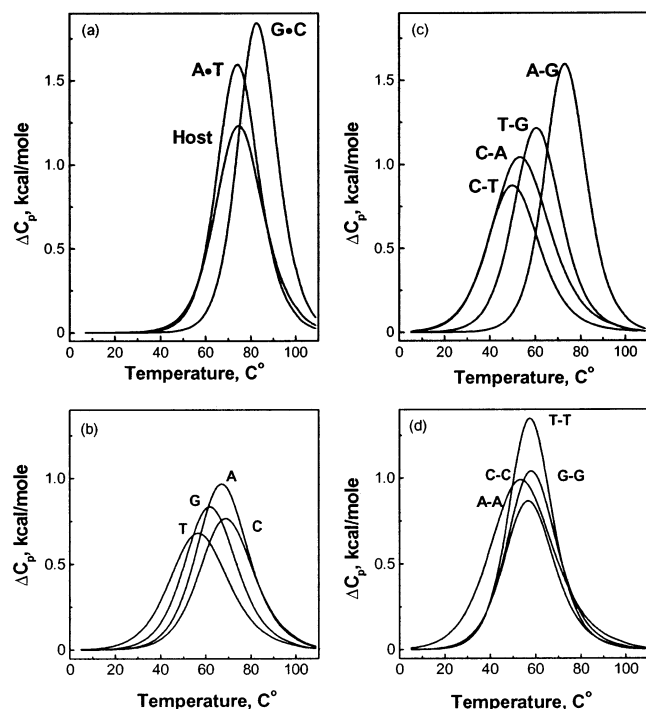


Figure 2. Heat capacity profiles of hairpins in 10 mM sodium phosphate buffer, 1 M NaCl, and 0.1 mM Na₂EDTA at pH 7 and 20 °C. (a) Hairpins with fully paired stems; (b) hairpins with bulges; (c) hairpins with heteromismatches; and (d) hairpins containing homomismatches.

capacities within the initial and final states. One exception is the G hairpin that showed an additional and small transition at lower temperatures (data not shown) because of the presence of degenerate states resulting from base migration. The T_M 's obtained from these melting experiments are listed in Table 1. Over this concentration range, the UV and DSC T_M 's for a given hairpin are within ± 1.1 °C, confirming the exclusive formation of single-stranded hairpins at low temperatures. The T_M 's range from 51 °C (C-T) to 83 °C (G•C). The "host" hairpin has a T_M of 75.3 °C, the inclusion of a dA•dT or dG•dC base pair yielded T_M 's of 74.6 °C and 83.2 °C, respectively. The inclusion of a bulge or a mismatch resulted with hairpins with lower thermal stability, $\Delta\Delta T_M$ of 6–25 °C, which varied according to the nature of the bulge or mismatch. The inclusion of a mismatch was most destabilizing with the only exception of the dA-dG mismatch that induced a $\Delta\Delta T_M$ of only 7.5 °C. Table 1 also shows the corresponding ΔH_{vH} and ΔH_{cal} parameters; these values are low and correspond to the unfolding of short stems of ~ 4 base-pair stacks, which further confirms their intramolecular formation. The average ΔH_{cal} value of ~ 32.0 kcal/mol is in good agreement with the value predicted for the melting of 2 dGC/dCG and 1 dCG/dCG base-pair stacks (~ 34.0 kcal) from DNA nearest-neighbor parameters.^{30,31} We obtained $\Delta H_{\text{vH}}/\Delta H_{\text{cal}}$ ratios of 0.95–1.06 for 13 of the 15 hairpins (see Table 1) allowing us to conclude that most hairpins melt in two-state transitions. The exceptions were the C-C and C-A hairpins that yielded much lower ratios suggesting the formation of additional helical states. This may be the result of base migration, yielding hairpins with two bulge bases.

Figure 3 shows the CD spectra at 20 °C; at this temperature the majority of the hairpins are completely folded. The overall shape of each spectrum corresponds to the semiconservative spectrum of a DNA molecule in the B-like conformation, that is, the negative and positive bands, with few exceptions, have similar magnitude. The main spectral variations among these

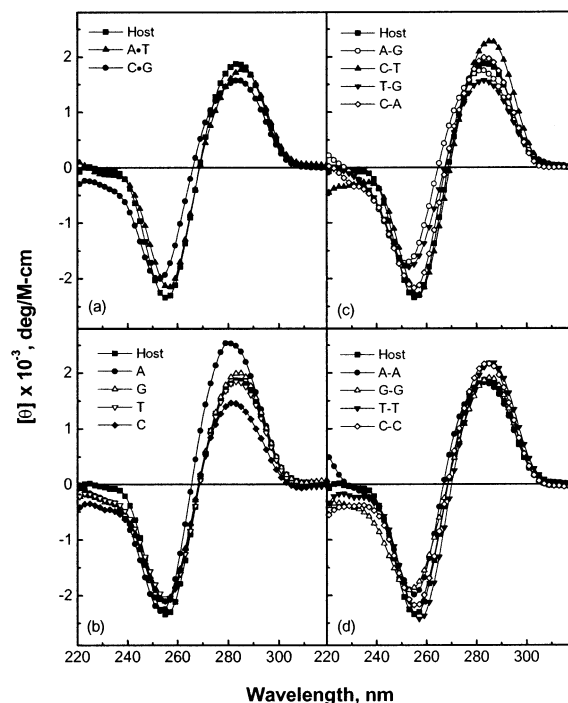


Figure 3. CD spectra of hairpins in 10 mM sodium phosphate buffer, 1 M NaCl, and 0.1 mM Na₂EDTA at pH 7 and 20 °C. (a) Hairpins with fully paired stems; (b) hairpins with bulges; (c) hairpins with heteromismatches; and (d) hairpins containing homomismatches.

molecules are in the magnitude and location of the spectral maxima and minima. The contribution of base-pair stacking interactions is determined by the magnitude of the negative band at ~ 255 nm, which ranges from -1800 to -2800 deg/M-cm. The sugar pucker and the single-strand content are reflected in the magnitude of the positive band. For proper comparisons, we have arbitrarily classified them into four groups: inclusion of W-C base pairs (Figure 3a), bulges (Figure 3b), the incorporation of heteromismatches (Figure 3c), and homomismatches (Figure 3d). All bulged hairpins have similar base-pair stacking interactions; however, the closer similarity of the host, G and T spectra suggest that these bulged bases are extrahelical while the A and C bulges are intrahelical. The T-T, C-C, C-T, and C-A hairpins have similar spectra to the host hairpin while it appears that the A-G, T-G, A-A, and G-G mismatches are less stacked and their minima are shifted to lower wavelengths.

Table 1 lists DSC enthalpies and entropies for the unfolding of each hairpin and the folding ΔG° at 20 °C (Figure 4a). These favorable ΔG°_{293} terms resulted from the characteristic partial compensation of a favorable enthalpy and unfavorable entropy terms (opposite signs of the values of Table 1). The favorable ΔH_{cal} values result from the formation of hydrogen bonds and base-pair stacks, whereas the unfavorable entropies indicate an ordering of the oligonucleotide and the uptake of counterions and water molecules. Overall, the placement of a bulge in the middle of the d(CG/GC) base-pair stack of the host hairpin results in an average destabilization of 2 kcal/mol, independent of the nature of the nucleotide inserted, as shown in Table 1. Their stability is in the following order: A > C > G > T, as shown in Figure 4a. This hierarchy differs from the previous studies^{32,33} and may be due to the different flanking base pairs examined. However, the magnitude of the enthalpy change is dependent on whether the bulge nucleotide is a purine or a pyrimidine. We obtained a decrease in the enthalpy of 7.0 kcal/mol (purines) and 10.8 kcal/mol (pyrimidines) but the entropy

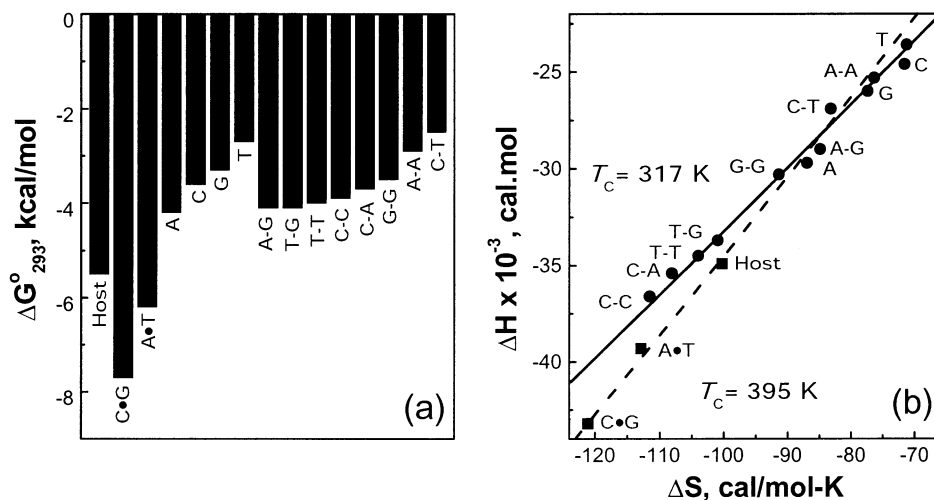


Figure 4. Thermodynamic profiles for the folding of hairpins in 10 mM sodium phosphate buffer, 1 M NaCl, and 0.1 mM Na₂EDTA at pH 7. (a) Stability of hairpins in terms of ΔG°_{293} ; (b) enthalpy–entropy compensations of hairpins, containing fully paired stems (dashed line), containing bulges and mismatch base pairs (solid line). The indicated T_c values correspond to the slopes from least-squares analysis of the lines.

terms of the pyrimidine bulges are more favorable. These findings are consistent with NMR investigations of bulged duplexes that have indicated that purines are stacked in the helix^{34,35} while pyrimidines are extrahelical.^{32,36} Previous investigations have shown that a DNA bulge has a destabilizing effect of 2.7–4.6 kcal/mol,^{32,35,37,38} which is higher than the range of 1.3–2.8 kcal/mol of this work. This comparison suggests that the overall thermodynamic effects are strongly dependent on the flanking sequence or base-pair stack where the lesion is placed and the nature of the bulge.

In terms of the magnitude of ΔG°_{293} (Table 1), the hairpins containing an additional W-C base pair or mismatch can be classified in four groups (Figure 4a). The most stable hairpins are the ones with exclusive Watson–Crick base pairs in their stems, C•G and A•T. The A-G, T-G, T-T, and C-C hairpins are on average 2.9 kcal/mol less favorable relative to the first group. The G-G and C-A are less stable by 3.4 kcal/mol and the least stable group, A-A and C-T, by 4.3 kcal/mol. The nature of these destabilizations is enthalpic and indicates primarily a loss of base-pair stacking interactions. Stacking interactions of mismatches are in general optimized in the pyrimidine–pyrimidine and purine–pyrimidine mismatches with the only exception of C-T, while there is a noticeable decrease in the enthalpy for the purine–purine mismatches.

The incorporation of mismatches in two base-pair stack environments, d(AA/TT) and d(TT/AA), of oligomer duplexes has been reported earlier.^{39,40} Comparisons among these three sets indicate that the T-G and A-G are very stable mismatches while the A-A is a destabilizing mismatch. The effects of all other mismatches on the stability of the host duplex depend on the flanking base sequence. In all the above cases, a stabilization of one mismatch relative to another is enthalpic in origin and arises from an inherent ability of a given base-pair stack to accommodate a particular mismatch. Overall, the magnitude of the destabilization in free energy terms is very similar in all three data sets, yet slightly less destabilizing in our set (by +1.8 kcal/mol). Relative to the host duplex, the average enthalpy change for the incorporation of a single mismatch is 9.8 kcal/mol (this work), 14.9 kcal/mol,³⁹ and 11.4 kcal/mol.⁴⁰ The origins of the differences may be explained in terms of the base-pair stack environment, the relative position of the mismatch in the oligomer duplex, and the overall thermodynamic stability of the DNA molecule. To date, a sufficient number of mismatched structures do not exist to enable us to make

structural-energetic correlations. However, the main factor determining the magnitude of the thermodynamic destabilization of a given mismatch is the enthalpy term, which depends on the thermodynamic stability of the flanking sequence or base-pair stack. This has been shown recently with homomismatches that were incorporated and compared in the 10 nearest-neighbors base-pair stacks.⁴¹

The favorable formation of a given hairpin at 20 °C yielded a partial enthalpy–entropy compensation, which is consistent with the expectation for any biochemical process. This reflects the combined first and second laws of thermodynamics for open systems, that is, the Gibbs relationship. However, to obtain a better picture of additional contributions in the incorporation of a W-C base pair, bulge, or mismatch, a plot of ΔH_{cal} versus ΔS_{cal} for the whole set of 15 hairpins is constructed and shown in Figure 4b. All points fall in a diagonal and a least-squares analysis demonstrated that they are linearly correlated with a slope of 357 K (c.c. = 0.987 and $\sigma = 961$), line not shown. Relative to the formation of the host hairpin, the more favorable hairpins with an extra W-C base pair fall at the bottom with a more negative enthalpy change and lower entropy because of the formation of an extra base-pair stack. The inclusion of bulges leads to less favorable hairpins that are spread out at the top third of the plot while the hairpins with mismatches are spread out over the top 70% of the plot. There are pairs or groups of hairpins with similar free energy terms but different enthalpy contributions (for example, A-G and T-G), indicating that the lower enthalpy is compensated with lower unfavorable entropy terms. The overall effects can arise from differences in configurational entropy, hydration, or counterion uptake. However, the contribution from the uptake of counterions can be ruled out because the differential counterion uptakes, equal to 0.55 ± 0.14 mol of Na⁺ per mole of hairpin, are similar (data not shown). In addition, incorporating an extra base or base pair to the 13 bases of the host hairpin is expected to result in favorable approximately similar entropy contributions to the configurational entropy. Therefore, the effects can be explained in terms of hydration differences, that is, the enthalpy differences are compensated with unfavorable hydration contributions, that is, immobilization of water by the folded hairpin. Overall, the slope (or compensating temperature, T_c) of 357 K is indicative of processes that are driven from solute–solvent interactions.⁴² Furthermore, better correlations are obtained when the hairpins are separated into two groups, see Figure 4b and Table 2. The

TABLE 2: Least-Squares Analysis of the ΔH – ΔS Compensations of Nucleic Acids^a

| nucleic acid | source | T_C (K) | corr. coeff. | σ |
|-----------------------------|-----------|-----------|--------------|----------|
| all hairpins | this work | 357 ± 16 | 0.987 | 961 |
| fully paired stems | this work | 395 ± 35 | 0.996 | 514 |
| bulges and mismatches | this work | 317 ± 11 | 0.994 | 498 |
| DNA nearest neighbors | ref 31 | 413 ± 39 | 0.966 | 657 |
| DNA nearest neighbors | ref 30 | 389 ± 41 | 0.957 | 513 |
| DNA mismatches ^b | ref 39 | 314 ± 9 | 0.997 | 541 |
| DNA mismatches | ref 40 | 281 ± 31 | 0.960 | 1379 |
| DNA homomismatches | ref 41 | 324 ± 7 | 0.999 | 179 |
| RNA nearest neighbors | ref 43 | 445 ± 25 | 0.987 | 411 |
| RNA/DNA nearest neighbors | ref 44 | 302 ± 23 | 0.961 | 763 |

^a The thermodynamic parameters used in these plots were all obtained in 10 mM sodium phosphate (or 10 mM sodium cacodylate), 1.0 M NaCl at pH 7.0; the only exception is the DNA mismatches of ref 40 that were in 0.1 M NaCl. ^b The values with higher uncertainties of this set were omitted from the least-squares analysis.

hairpins with lesions, bulges, and mismatches fall in a straight line with a slope of 317 K (c.c. = 0.996 and σ = 514) and the hairpins with fully paired stems yielded a much higher slope of 395 K (c.c. = 0.997 and σ = 498). The T_C of 317 K for the hairpins with lesions is similar to the T_C found in protein unfolding, in which hydrophobic or structural water plays a key role.⁴² Furthermore, volume change measurements for the single incorporation of lesions and W-C base pairs into duplex DNA show an immobilization of structural and electrostricted water, respectively.^{37,45,46} We would like to suggest that structural water participates in the enthalpy–entropy compensation of the hairpins with lesions while electrostricted water participates in the folding of hairpins with fully paired stems. One possible explanation for this behavior is that the immobilization of these two types of water is accompanied by opposite heat contributions. Moreover, similar plots with published data of other laboratories, as shown in Table 2, result in enthalpy–entropy compensations (and T_C 's) in excellent agreement with the results reported here.

Finally, Table 2 also shows a T_C of 445 K for the RNA nearest neighbors;⁴³ this is due to their lower hydration level⁴⁷ because their A conformation is much less dependent on the activity of water. The nearest neighbors of the RNA–DNA hybrids⁴⁴ yielded a T_C of 302 K; their overall hydration is comparable to that of RNA duplexes.⁴⁷ However, these duplexes fold in a mixed A/B conformation yielding perhaps a partial exposure of the bases to the solvent, which immobilizes structural water.

Conclusions

We used melting protocol to study the helix-coil transition of oligomers and demonstrated the exclusive formation of single-stranded hairpins at low temperatures. The incorporation of a lesion in the middle of a d(CG/CG) base-pair stack lowers its thermal stability, which is the result of the loss of favorable enthalpy interactions^{39–41} and immobilization of structural water.^{37,46,47} The magnitude of these effects depends on the nature of the base and of the local environment of the neighboring base pairs.^{39–41} The results are in very good agreement with those obtained using DNA bimolecular duplexes as host molecules and should help in predicting the stability of DNA secondary structures. It is quite interesting that although there are several consistent trends among the various thermodynamic sets, there appears to be a discrepancy about their absolute thermodynamic values. It becomes evident then that

the actual values depend on the nature of the lesion, flanking base pairs, overall oligomer stability, and extrapolation of their thermodynamic parameters to a common reference temperature. However, all results yielded similar enthalpy–entropy compensations indicating that a common and underlying phenomenon unifies all trends. We suggest that the differential enthalpy contributions of each lesion are compensated with different degrees of unfavorable hydration contributions. Furthermore, the differences in the enthalpy–entropy compensation, that is, compensating temperatures, observed for hairpins with fully paired stems and hairpins with lesions can be explained by the participation of different types of water. The incorporation of canonical W-C base pairs immobilize electrostricted water while the incorporation of lesions immobilize structural water.

Acknowledgment. This work was supported by Grant GM-42223 from the National Institutes of Health and a graduate assistantship (R.S.) from the Nebraska Research Initiative at UNMC.

References and Notes

- (1) Lilley, D. M. J. *Proc. Natl. Acad. Sci. U.S.A.* **1980**, *77*, 6468–6472.
- (2) Maniatis, T.; Ptanshe, M.; Mackman, K.; Kleid, D.; Flashman, S.; Jeffrey, A.; Maurer, R. *Cell* **1975**, *5*, 109–113.
- (3) Müller, U. R.; Fitch, W. M. *Nature* **1982**, *298*, 582–585.
- (4) Alastair, I. H.; Bowater, R.; Fareed, A.; Lilley, D. M. J. *Biochim. Biophys. Acta* **1992**, *1131*, 1–15.
- (5) Chattopadhyaya, R.; Ikuta, S.; Grzewskiowiak, K.; Dickerson, R. E. *Nature* **1988**, *334*, 175–179.
- (6) Chattopadhyaya, R.; Brzewskiowiak, K.; Dickerson, R. E. *J. Mol. Biol.* **1990**, *211*, 189–210.
- (7) Hare, D. R.; Reid, B. R. *Biochemistry* **1986**, *25*, 5341–5350.
- (8) Hilbers, C. W.; Haasnoot, C. A. G.; de Bruin, S. H.; Joordens, J. J. M.; van der Marel, G. A.; van Boom, J. H. *Biochimie* **1985**, *67*, 685–695.
- (9) Gupta, G.; Garcia, A. E.; Hiriyanna, K. T. *Biochemistry* **1993**, *32*, 948–960.
- (10) Haasnoot, C. A. G.; den Hartog, J. H. J.; de Rooij, J. F. M.; van Boom, F. H.; Altona, C. *Nucleic Acids Res.* **1980**, *8*, 169–181.
- (11) Wemmer, D. E.; Chou, S. H.; Hare, D. R.; Reid, B. R. *Nucleic Acids Res.* **1985**, *13*, 3755–3772.
- (12) Williamson, J. R.; Boxer, S. G. *Biochemistry* **1989a**, *28*, 2819–2831.
- (13) Doktycz, M. J.; Goldstein, R. F.; Paner, R. M.; Gallo, F. J.; Benight, A. S. *Biopolymers* **1992**, *32*, 849–864.
- (14) Paner, T. M.; Amaratunga, M.; Benight, A. S. *Biopolymers* **1992**, *32*, 881–892.
- (15) Garcia, A. E.; Gupta, G.; Sarma, M. H.; Sarma, R. H. *J. Biomol. Struct. Dyn.* **1988**, *6*, 525–542.
- (16) Antao, V. P.; Tinoco, I. J. *Nucleic Acids Res.* **1992**, *20*, 819–824.
- (17) Rentzeperis, D.; Alessi, K.; Marky, L. A. *Nucleic Acids Res.* **1993**, *21*, 2683–2689.
- (18) Senior, M.; Jones, R. A.; Breslauer, K. J. *Proc. Natl. Acad. Sci. U.S.A.* **1988**, *85*, 6242–6246.
- (19) Erie, D. A.; Sure, A. K.; Breslauer, K. J.; Jones, R. A.; Olson, W. K. *Biochemistry* **1993**, *32*, 436–454.
- (20) Brown, T. C.; Jiricny, J. *Genome* **1989**, *31*, 578–583.
- (21) Goodman, M.; Creighton, S.; Bloom, L.; Petruska, J. *Crit. Rev. Biochem. Mol. Biol.* **1993**, *28*, 83–162.
- (22) Streisinger, G.; Okada, Y.; Emrich, J.; Newton, J.; Tsugita, A.; Terzaghi, E.; Inouye, M. *Cold Spring Harbor Symp. Quant. Biol.* **1966**, *31*, 77–84.
- (23) Lewin, B. *GENES VII*; Oxford University Press: New York, 2000.
- (24) Frank, H. S.; Evans, M. W. *J. Phys. Chem.* **1945**, *13*, 507–532.
- (25) Kauzman, W. *Adv. Protein Chem.* **1959**, *14*, 1–63.
- (26) Millero, F. J. *J. Chem. Rev.* **1971**, *71*, 147–176.
- (27) Caruthers, M. H. In *Chemical and Enzymatic Synthesis of Gene Fragments*; Gassen, H. G., Lang, A., Eds.; Verlag Chemie: Weinheim, Germany, 1982.
- (28) Marky, L. A.; Canuel, L.; Jones, R. A.; Breslauer, K. J. *Biophys. Chem.* **1981**, *13*, 141–149.
- (29) Marky, L. A.; Breslauer, K. J. *Biopolymers* **1987**, *26*, 1601–1620.
- (30) SantaLucia, J. J.; Allawi, H. T.; Seneviratne, A. *Biochemistry* **1996**, *35*, 3555–3562.
- (31) Breslauer, K. J.; Frank, R.; Blöcker, H.; Marky, L. A. *Proc. Natl. Acad. Sci. U.S.A.* **1986**, *83*, 3746–3750.

- (32) Le Blanc, K. A.; Morden, K. M. *Biochemistry* **1991**, *30*, 4042–4047.
- (33) Zhu, J.; Wartell, R. M. *Biochemistry* **1999**, *38*, 15986–15993.
- (34) Kalnik, M. W.; Norman, D. G.; Swann, P. F.; Patel, D. J. *J. Biol. Chem.* **1989**, *264*, 3702–3712.
- (35) Patel, D. J.; Kozowski, A.; Marky, L. A.; Rice, J. A.; Broka, C.; Itakura, K.; Breslauer, K. J. *Biochemistry* **1982**, *21*, 445–451.
- (36) Kalnik, M. W.; Norman, D. G.; Zagorski, M. G.; Swann, P. F.; Patel, D. J. *Biochemistry* **1989**, *28*, 294–303.
- (37) Zieba, K.; Chu, T. M.; Kupke, D. W.; Marky, L. A. *Biochemistry* **1991**, *30*, 8018–8025.
- (38) Woodson, S. A.; Crothers, D. M. *Biochemistry* **1988**, *27*, 3130–3141.
- (39) Aboul-ela, F.; Koh, D.; Tinoco, I. J. *Nucleic Acids Res.* **1985**, *13*, 4811–4824.
- (40) Gaffney, B. L.; Jones, R. A. *Biochemistry* **1989**, *28*, 5881–5889.
- (41) Peyret, N.; Seneviratne, A.; Allawi, H. T.; SantaLucia, J. J. *Biochemistry* **1998**, *38*, 3468–3477.
- (42) Lumry, R.; Rajender, S. *Biopolymers* **1970**, *9*, 1125–1227.
- (43) Freier, S. M.; Kierzed, R.; Jaeger, J. A.; Sugimoto, N.; Caruthers, M. H.; Neilson, T.; Turner, D. *Proc. Natl. Acad. Sci. USA* **1986**, *83*, 9373–9377.
- (44) Sugimoto, N.; Nakano, S.-i.; Katoh, M.; Matsumura, A.; Nakamuta, H.; Ohmichi, T.; Yoneyama, M.; Sasaki, M. *Biochemistry* **1995**, *34*, 11211–11216.
- (45) Zhong, M.; Marky, L. A.; Kallenbach, N. R.; Kupke, D. W. *Biochemistry* **1997**, *36*, 2485–2491.
- (46) Marky, L. A.; Kupke, D. W. *Methods Enzymol.* **2000**, *323*, 419–441.
- (47) Kankia, B. I.; Marky, L. A. *J. Phys. Chem. B* **1999**, *103*, 8759–8767.